

NAL PROPOSAL # 313  
Spokesman:  
H. A. Neal  
Dept. of Physics  
Indiana University  
Bloomington, Indiana 47401  
Tel. 812-337-4089

POLARIZATION IN p-p ELASTIC, INELASTIC AND INCLUSIVE  
REACTIONS AT NAL ENERGIES

G. W. Abshire, B. B. Brabson, R. R. Crittenden, A. Dzierba, S. Gray,  
R. M. Heinz, J. E. Mott, H. A. Neal, and D. R. Rust

Department of Physics  
Indiana University  
Bloomington, Indiana 47401

ABSTRACT

We propose to utilize the expanded C-0 Internal Target Laboratory to measure the polarization parameter in p-p elastic scattering at momenta from 30 to 400 GeV/c for  $|t|$  values between .2 and 2.0 (GeV/c)<sup>2</sup>. We plan also to study the proton polarization in the processes  $p + p \rightarrow N^* + p$  and  $p + p \rightarrow p + X$ . The recoil spectrometer of experiment 198 would be employed to select the desired events. This spectrometer would be followed by a proportional chamber carbon polarimeter, which would allow the recoil proton polarization to be determined to an accuracy of  $\pm 1$  to 2% from an analysis of the proton double scattering distribution.

## I. Introduction

We propose herein an experiment in the expanded C-0 Internal Target Laboratory to measure the polarization parameter in p-p elastic scattering at momenta between 30 and 400 GeV/c for  $|t|$  values between .2 and 2.0 (GeV/c)<sup>2</sup>, and to study the final state proton polarization in the processes  $p + p \rightarrow N^* + p$  and  $p + p \rightarrow p + X$ . The recoil spectrometer of experiment 198 would be utilized to select the desired events. The polarization of the recoil protons would be determined to an accuracy of  $\pm 1$  to 2% from the azimuthal asymmetry exhibited in the proton double scattering in a carbon analyzer, which is located downstream of the spectrometer. Over the  $t$  range of interest, sufficient missing mass resolution is attained solely from the determination of the scattering angle and momentum analysis of the recoil proton.

## II. Physics Interest

### A. p-p Elastic Scattering Polarization

On the basis of present trends it is reasonable to expect that polarization effects at NAL energies will be quite small. However, actual quantitative extrapolations of fits to the present data predict that experimentally detectable elastic polarizations will persist even at momenta near 200 GeV/c. If this is true then we would have, for the first time, the opportunity to make a non-trivial map of the energy dependence of the fixed  $t$  polarization over an enormous energy range. This dependence would provide, for example, a definite test of the Regge theory.

In the simple Regge theory the polarization in p-p elastic scattering arises from the pairwise interference of the participating Regge trajectories. Muzinich<sup>1</sup> has shown that, if one assumes that  $s$  is large ( $\gg m_N^2$ ) and that  $|t|$  is small ( $\ll s$ ), the following result obtains:

$$P(t) = A(t) \left( \frac{s}{s_0} \right)^{\alpha_R(t) - \alpha_P(t)} \quad (I)$$

Here  $\alpha_R(t)$  is the effective Regge trajectory corresponding to the trajectory with the quantum numbers of the  $p - \bar{p}$  channel that lies closest to the Pomeron trajectory  $\alpha_P(t)$ .  $A(t)$  incorporates the residue and signature factors but is independent of  $s$ . Consequently, at fixed  $t$  the elastic polarization is expected to decrease as some power of  $s$ . Present polarization data tend to support this hypothesis, although the effective Regge trajectory does not seem to correspond to one containing known particles. Figures 1-3 show polarization data at three values of  $t$  as a function of  $s$ . The solid circles represent existing data which were used to determine the least squares fit for the amplitude and slope in Eq. I. The best fit is shown as the curve in the respective figure. The open circles (which we have positioned arbitrarily along this curve) are points that this experiment would measure. This experiment should permit the determination of the effective Regge trajectory over a wide range of  $t$  values.

The salient characteristics<sup>2</sup> of present high energy  $p$ - $p$  polarization data are illustrated in Fig. 4. There exists a maximum in the polarization near  $t = -.3 \text{ (GeV/c)}^2$ , a minimum near  $t = -.8 \text{ (GeV/c)}^2$ , and another maximum near  $t = -1.7 \text{ (GeV/c)}^2$  followed by a minimum near  $t = -2.5 \text{ (GeV/c)}^2$ . It will be of interest to determine if these  $t$ -dependent features persist at NAL energies.

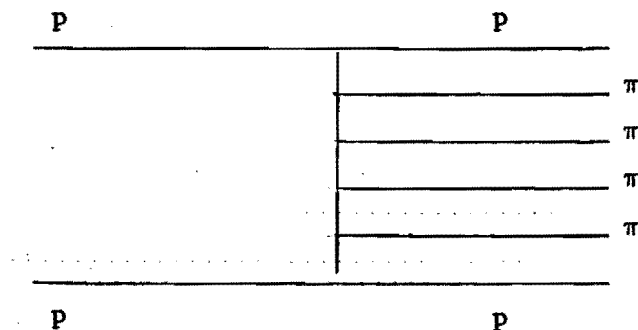
The  $t$ -dependent structure in the polarization data is expected in optical models such as the model of Chu and Hendry<sup>3,4</sup> as shown in Fig. 4. Structure, near  $-t = 1.3 \text{ (GeV/c)}^2$ , consistent with an optical effect is observed in the elastic differential cross section at momenta  $\gtrsim 10 \text{ GeV/c}$ , and is quite pronounced at ISR energies. If indeed an optical diffraction picture becomes valid at  $p \gtrsim 10 \text{ GeV/c}$ , one would expect to see a continuation of the  $t$ -independent dip structure in the polarization as the energy is increased.

### B. Polarization in $N^*$ Production

To our knowledge no polarization studies have been made of the recoil proton in  $N^*$  production processes. We propose to measure the proton polarization in  $p + p \rightarrow N^* (1520) + p$  and  $p + p \rightarrow N^* (1688) + p$  at several  $t$  values in the range  $.2 < |t| < 1.0 \text{ (GeV/c)}^2$ . Accurate polarization data for these reactions will provide stringent tests for various production hypotheses. The yields for these processes are expected to be of the same order as that for elastic scattering.

### C. Polarization in the Inclusive Reaction $p + p \rightarrow p + X$

All first generation models for the inclusive process  $p + p \rightarrow p + X$  predict zero polarization for the final state proton. However, new evidence for strong correlations amongst the final state particles certainly allows for the possibility of leading particle polarization. In the multi-peripheral diagram shown below the  $x = -1$  proton may be preferentially produced as the final state proton in an elastic  $\pi p$  scattering, which occurs at very low subenergy. At low subenergies the  $\pi p$  polarization can be large and, even with the dilution due to the contributions from  $\pi^+ p$ ,  $\pi^- p$  and  $\pi^0 p$  processes, measurable polarizations may still survive. Observation of a finite polarization in the inclusive process would certainly have a significant impact on the evaluation of the various proposed mechanisms.



### III. Experimental Technique

The polarization of the recoil proton will be determined to an accuracy of  $\pm 1$  to 2% with a carbon polarimeter which is located downstream of the recoil spectrometer of experiment 198, as shown in Figs. 5 and 6. The analyzer consists of a carbon block with transverse dimensions of 19" X 14" with a thickness chosen between  $\frac{1}{2}$ " and 3" depending on the proton energy being studied. The carbon is preceded and followed by a group of 8 multiwire proportional chambers. The polar ( $\theta$ ) and azimuthal ( $\phi$ ) angles associated with the second scatter in the carbon will be recorded for each event. An analysis of the distribution in  $\phi$  will allow the polarization to be determined, since the carbon analyzing power for the proton kinetic energies of interest are known from previous measurements (or will be determined in an upcoming calibration run with the ZGS polarized beam.)

The distributions corresponding to the copious small angle second scatters will be valuable in continuously monitoring the polarimeter alignment. These events, the double scattered meson events, and events accumulated with the carbon block removed will form a powerful tool for eliminating the effect of any residual systematic errors.

The analyzing efficiency for the polarimeter will be  $\approx .005$  at all proton kinetic energies covered by the experiment. (This corresponds to the fraction of the protons incident on the carbon block which scatter into the laboratory polar angle region  $6^\circ < \theta_L < 22^\circ$ . Scatters outside this region are not useful for polarization determination.) The effective analyzing power  $\overline{A \cos \phi}$  will be  $\approx .2$ . These numbers are based on the known properties of similar polarimeters which have been utilized in recent experiments (see Refs. 5 and 6).

The status of the polarimeter chambers would be recorded for each spectrometer trigger. To minimize chances for instrumental biases no trigger counters

will follow the carbon analyzer. A dual processor PDP-15 would be used to record, monitor, and analyze all aspects of the polarimeter and spectrometer data.

#### IV. Rates

We anticipate that at the time of the experiment the following yield parameter values will be typical:

<u>Parameter</u>	<u>Value</u>
NAL circulating intensity	$2 \times 10^{13}$ protons/sec.
jet target density	$8 \times 10^{-7}$ g/cm <sup>3</sup>
effective target length	1.1 cm
duration of jet pulse	200 ms
target traversals by beam proton during jet pulse	$10^4$

These specifications correspond to a target of  $N_t = 5.3 \times 10^{17}$  protons/cm<sup>2</sup> and an effective beam intensity of  $N_b = 2 \times 10^{17}$  protons per jet pulse. The number of elastic events per jet pulse is then

$$N = N_b N_t \frac{d\sigma}{dt} \Delta t \frac{\Delta\phi}{2\pi} = 1.06 \times 10^{35} \frac{d\sigma}{dt} \Delta t \frac{\Delta\phi}{2\pi} / \text{jet pulse}$$

The value of  $\frac{d\sigma}{dt}$  can be estimated from the existing cross section data. The values of  $\Delta t$  and  $\Delta\phi$  are chosen to correspond to the size of the carbon block at 30 ft. from the internal target as seen through the E-198 recoil spectrometer. If we utilize 2 jet pulses per machine cycle, our elastic event rate will vary from  $\sim 130/\text{burst}$  at  $t = -2$  (GeV/c)<sup>2</sup> to  $\sim 10^4/\text{burst}$  at  $t = -.2$  (GeV/c)<sup>2</sup>.

We propose to measure the polarization at the  $s$  and  $t$  values shown in Table I. This table also shows the projected running times required to obtain the desired statistical error  $\Delta P$  in the polarization. The effective analyzing

power, analyzing efficiency and  $t$  bin width are given in Table II. As can be seen, we propose to determine the elastic polarization at  $\sim 13$   $|t|$  values between .2 and 2.0 (GeV/c)<sup>2</sup> at each of  $\sim 12$   $s$  values between  $s = 63$  and 752 (GeV)<sup>2</sup>. We estimate that this will require 1500 hours of machine time.

In the  $N^*$  studies we would concentrate on the low  $t$  region ( $|t| < 1$  (GeV/c)<sup>2</sup>) and consequently, if the present similarity in the elastic and  $N^*(1520)$ ,  $N^*(1688)$  cross sections continues to hold, only 500 hrs. would be required. In addition, because of high yields in the region of interest, the inclusive polarization survey near  $x = -1$  could be completed in about 100 hrs. Our interest in pursuing the latter studies will, of course, depend on the results of the initial survey.

In Table III we have compared the effectiveness of the carbon analyzer technique with that of polarized targets for the study of the elastic proton polarization. We observe that, for a given amount of running time, the carbon technique should in principle result in a  $\sqrt{2}$  smaller statistical error. Also, of course, the  $N^*$  and inclusive studies are really only possible with the carbon analyzer technique.

## V. Background, Resolution

The background and mass resolution pertinent to the proposed measurements have been exhaustively treated in proposal 198 and will not be reproduced here. Over our  $t$  range the background trigger rates are expected to be totally negligible.

## VI. Preparations

The fabrication of the polarimeter and the writing of all necessary monitoring software routines could be accomplished within a six-month period following the approval of the experiment. Our group would be available to assist in the assembly of the 198 spectrometer.

## REFERENCES

1. I. J. Muzinich, Phys. Rev. Letters 9, 475 (1962).
2. G. W. Abshire, C. M. Ankenbrandt, R. R. Crittenden, R. M. Heinz, K. Hinotani, H. A. Neal, and D. R. Rust, Phys. Rev. Letters 32, 1261 (1974).
3. S.-Y. Chu and A. W. Hendry, Phys. Rev. D6, 190 (1972).
4. T.-Y. Cheng, S.-Y. Chu, and A. W. Hendry, Phys. Rev. D7, 86 (1973).
5. P. H. Surko, Lawrence Radiation Laboratory Report UCRL-19451.
6. G. W. Abshire, C. M. Ankenbrandt, B. B. Brabson, R. R. Crittenden, R. M. Heinz, K. Hinotani, J. E. Mott, H. A. Neal, and A. J. Pawlicki, Phys. Rev. D9, 003 (1974).
7. M. Borghini, L. Dick, J. C. Olivier, H. Aoi, D. Cronenberger, G. Grégoire, Z. Janout, K. Kuroda, A. Michalowicz, M. Poulet, D. Sillou, G. Bellettini, P. L. Braccini, T. Del Prete, L. Foá, P. Laurelli, G. Sanguinetti, and M. Valdata, Phys. Letters 36B, 493 (1971).

### Running Times\*

[illegible]

TABLE I (Cont'd.)

Running Times\*

.8		.9		1.0		1.1		1.2		1.6		2.0	
T	$\Delta P$	T	$\Delta P$	T	$\Delta P$	T	$\Delta P$	T	$\Delta P$	T	$\Delta P$	T	$\Delta P$
3	.0120	3	.0120	7	.0125	15	.0125	28	.0130	27	.0140	21	.0150
3	.0120	3	.0120	8	.0125	17	.0125	31	.0130	35	.0140	25	.0150
3	.0120	3	.0120	9	.0125	18	.0125	34	.0130	43	.0140	29	.0150
3	.0120	3	.0125	10	.0125	18	.0130	37	.0130	55	.0140	34	.0150
3	.0120	3	.0125	10	.0125	20	.0130	41	.0130	72	.0140	42	.0150
3	.0125	3	.0125	10	.0130	20	.0130	41	.0135	81	.0145	44	.0155
3	.0125	3	.0130	10	.0130	20	.0135	46	.0135	102	.0145	52	.0155
3	.0130	3	.0130	10	.0135	23	.0135	47	.0140	121	.0150	59	.0160
3	.0130	3	.0135	11	.0135	23	.0140	52	.0140	151	.0150	69	.0160
3	.0135	3	.0140	11	.0140	23	.0145	54	.0145	172	.0155	77	.0165
3	.0140	3	.0145	11	.0145	24	.0150	58	.0150	208	.0160	85	.0170
3	.0150	3	.0150	10	.0155	24	.0155	56	.0160	218	.0170	86	.0180
36		36		117		245		525		1290		623	

\*Note the running time is in hours and assumes 600 pulses/hour and a 60% duty cycle. The total is ~3000 hours; however, with two jets of 200 ms each per pulse the real running time is 1500 hours.

TABLE II

$-t$ (GeV/c) <sup>2</sup>	$\Delta t$ <sup>(a)</sup>	Effective Analyzing Power A <sup>(b)</sup>	Analyzing Efficiency <sup>(c)</sup>
.2	.055	.3	.023
.3	.069	.3	.008
.4	.082	.3	.005
.5	.093	.3	.008
.6	.105	.3	.008
.7	.117	.3	.008
.8	.127	.3	.011
.9	.138	.3	.011
1.0	.148	.2	.011
1.1	.159	.2	.015
1.2	.170	.2	.015
1.6	.211	.2	.018
2.0	.254	.2	.022

(a)  $\Delta t$  has a slight dependency on the s value.

(b) Ref. 5 has  $A > .3$  if the proton kinetic energy is less than 500 MeV and  $A > .2$  otherwise.

(c) Analyzing efficiency =  $t_c E_{ds}$  where  $t_c$  = number inches of carbon ( $\frac{1}{2}$ " to 3") and  $E_{ds}$  = fraction of protons that double scatter between  $6^\circ$  and  $22^\circ$  after going through 1" of carbon (determined in experiment of Ref. 6).

TABLE III

Comparison of Effectiveness of the Carbon Analyzer Technique  
and the Polarized Target Technique at  $-t = 1.5 \text{ (GeV/c)}^2$

Parameter	Polarized Target Experiment In a Secondary Beam	Carbon Analyzer Experiment With a Jet Gas Target
Maximum beam intensity	$10^7$ protons per pulse	$4 \times 10^{17}$ protons per pulse
Target proton area density	$6.5 \times 10^{23}$ protons/cm <sup>2</sup>	$5.3 \times 10^{17}$ protons/cm <sup>2</sup>
Luminosity (L)	$6.5 \times 10^{31}$ /cm <sup>2</sup>	$2.12 \times 10^{35}$ /cm <sup>2</sup>
Analyzing Power (A)	.70	.20
Azimuthal Acceptance ( $\Delta\phi$ )	.35 rad	.13 rad
Analyzing Efficiency ( $\epsilon$ )	1.0	.018
Effectiveness Parameter: ( $E \equiv L\Delta\phi A^2\epsilon$ )	$1.1 \times 10^{31}$	$2.0 \times 10^{31}$

# CAPTIONS

Figure 1. Polarization vs.  $s$  at  $t = -.4 \text{ (GeV/c)}^2$ . The solid circles are existing data. The curve shown is the best least squares fit to the existing data. The open circles are arbitrarily placed (in polarization) points that this experiment will measure.

Figure 2. Same as 1 except at  $t = -1.0 \text{ (GeV/c)}^2$ .

Figure 3. Same as 1 except at  $t = -1.6 \text{ (GeV/c)}^2$ .

Figure 4. Polarization vs.  $-t$  near 12 GeV/c. The triangles are data at 10 GeV/c from Borghini et al.<sup>7</sup>; the circles are from Abshire et al.<sup>2</sup> The curve is a fit using the Chu-Hendry optical model.

Figure 5. Experimental setup from NAL experiment 198 with our polarimeter shown at the downstream end.

Figure 6. Enlarged view of the polarimeter only. Each chamber represents both horizontal and vertical coordinates.

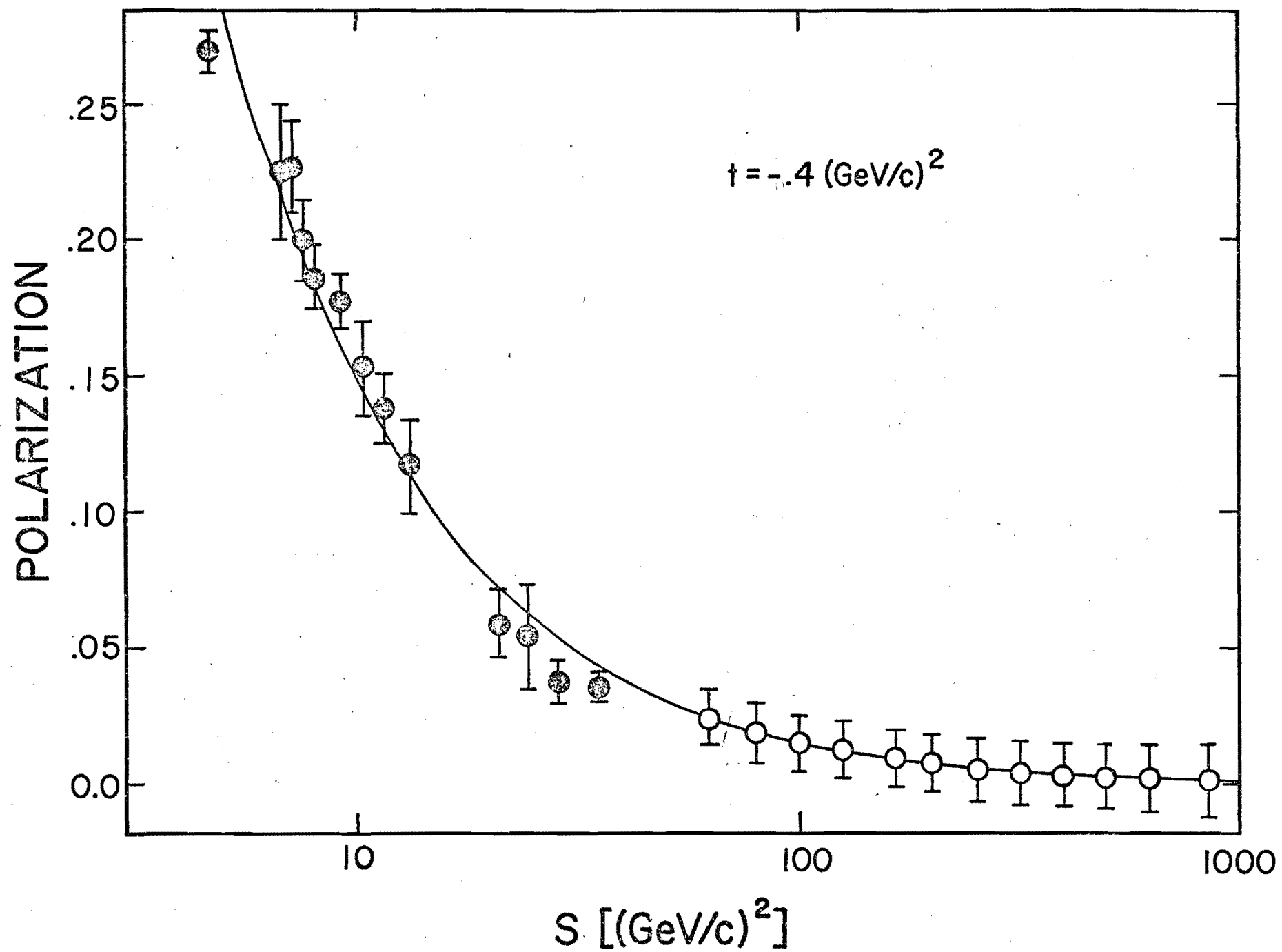


Figure 1

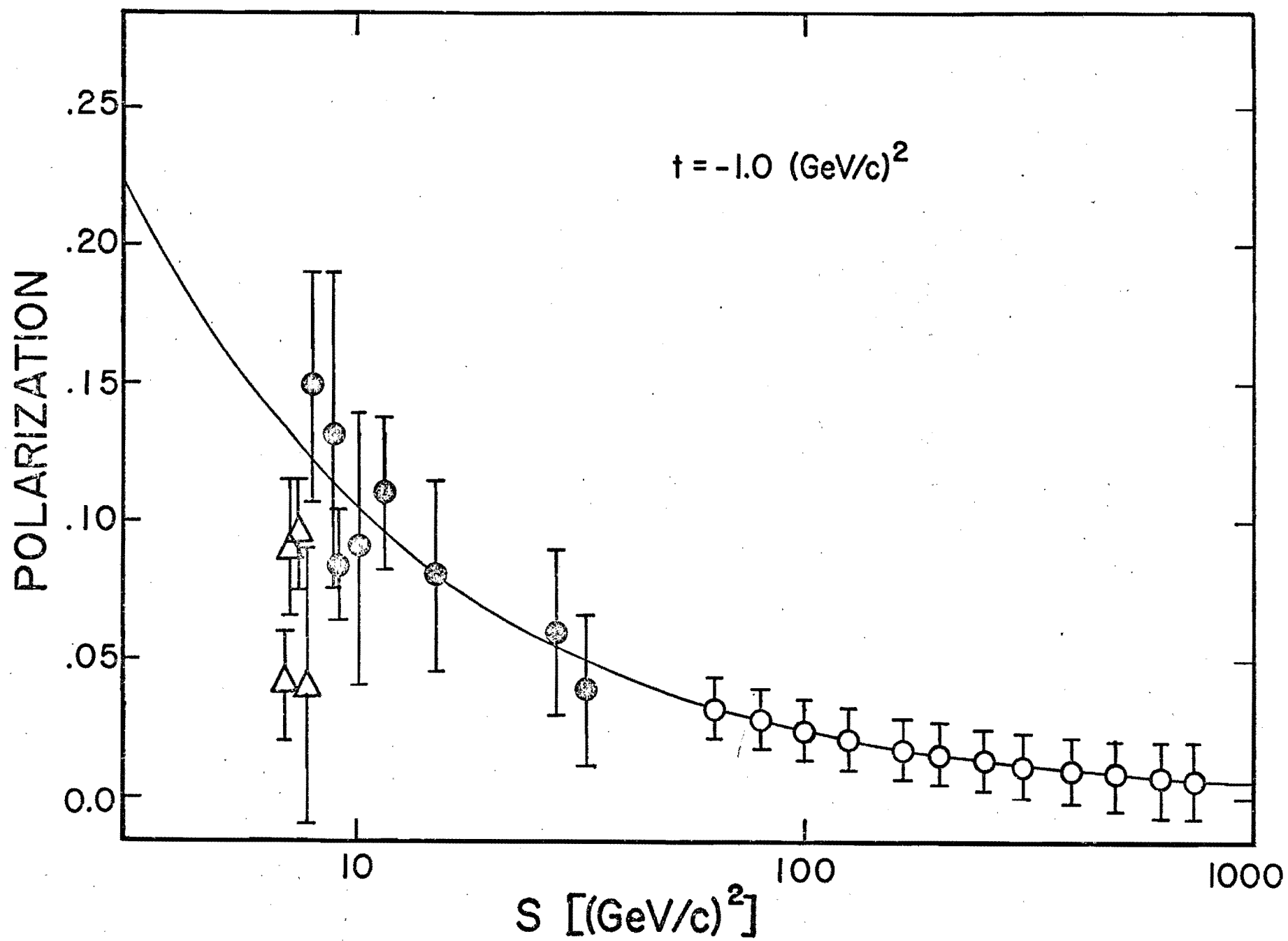


Figure 2

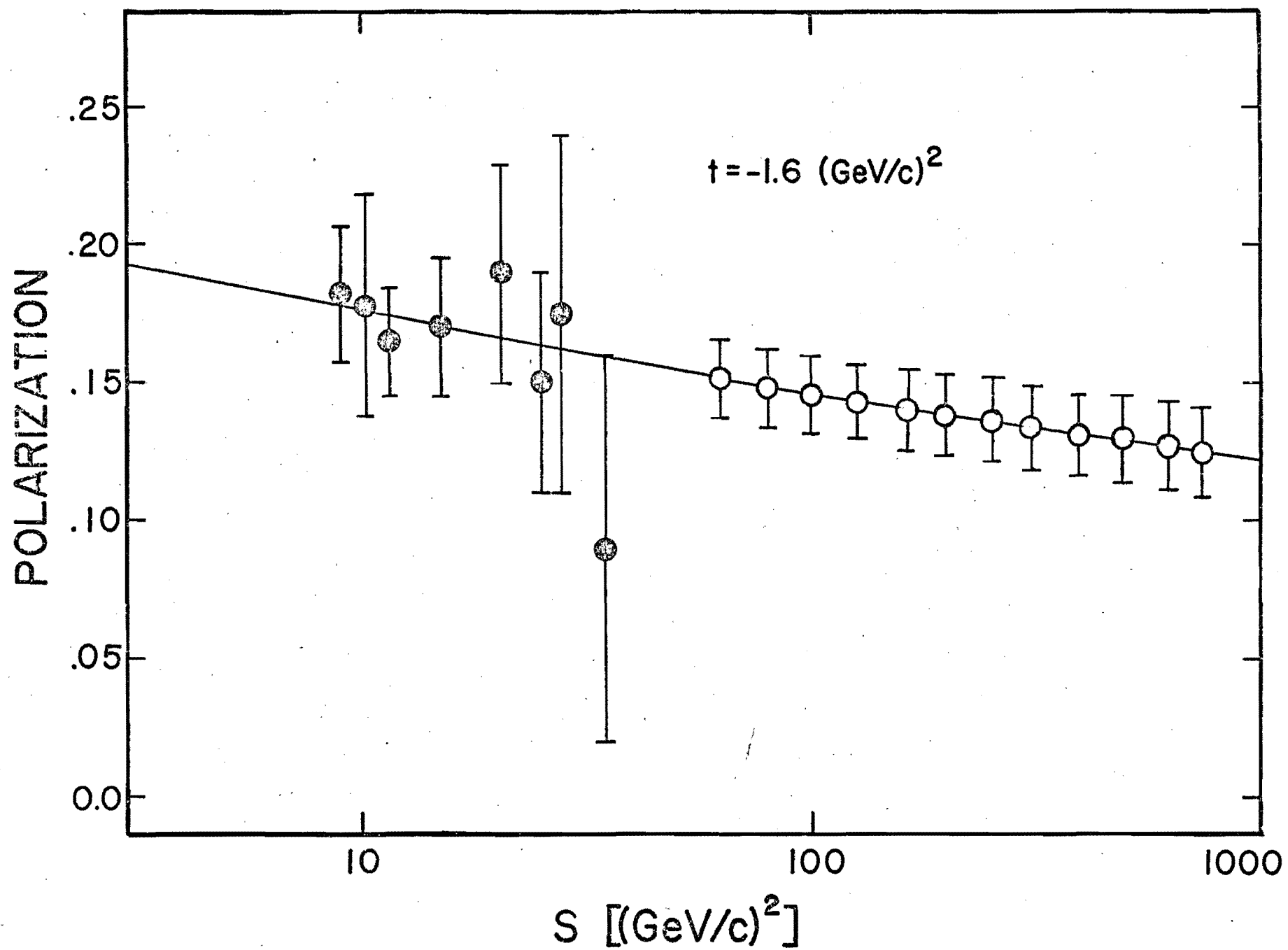


Figure 3

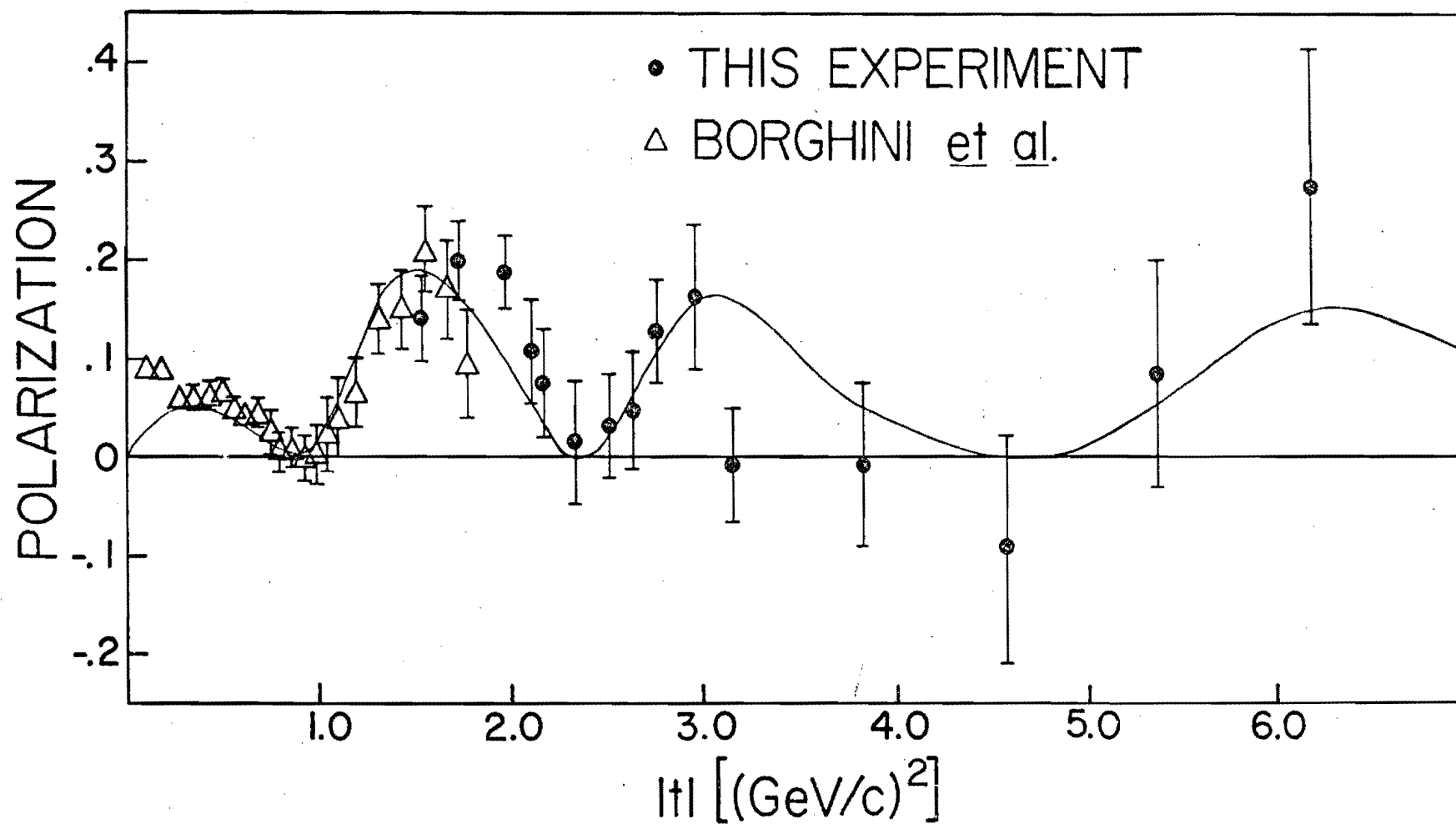
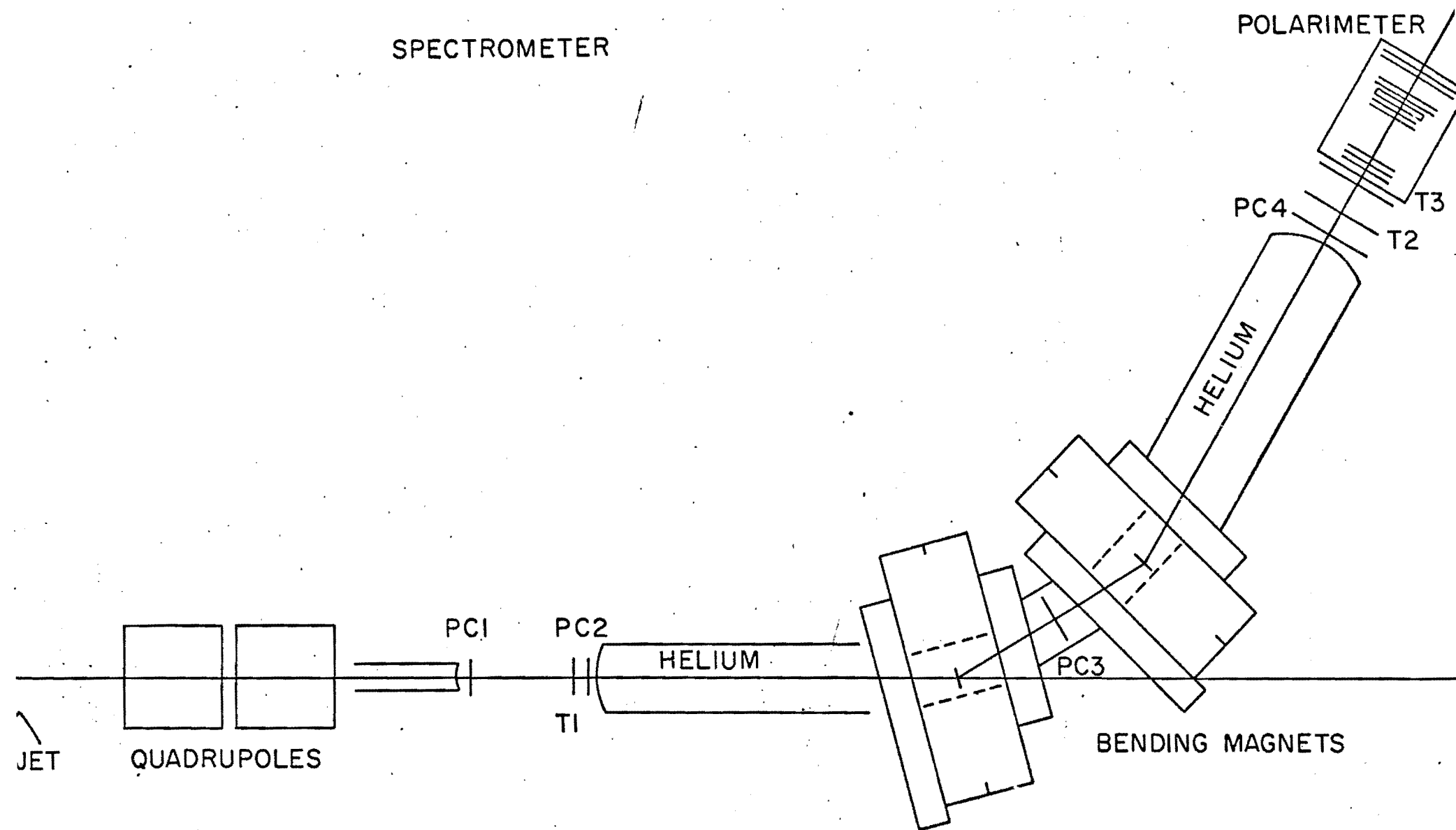


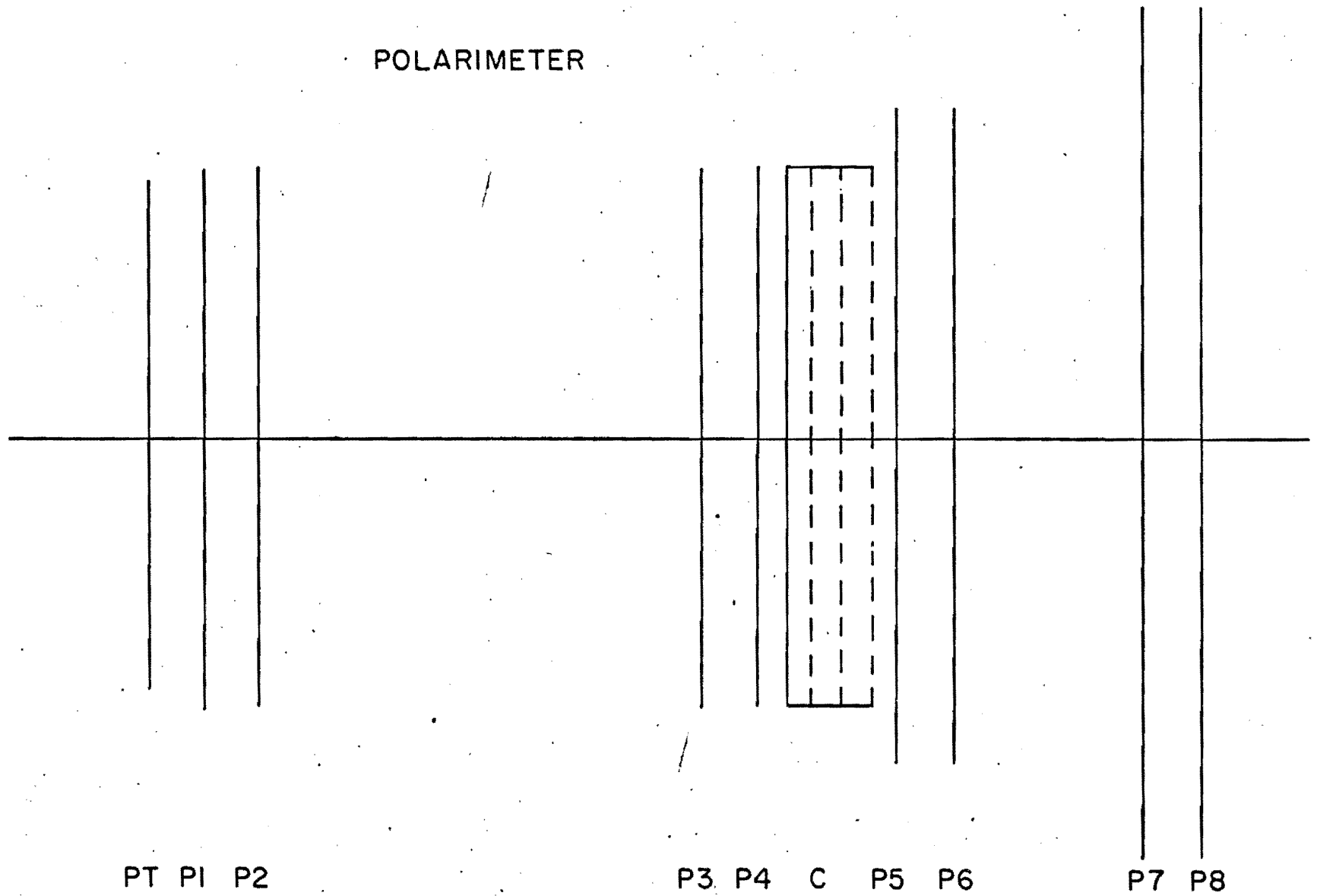
Figure 4



SCALE: 1/4" = 1"

Figure 5

POLARIMETER



SCALE:  $\frac{3}{16}'' = 1''$